Effects of the Platelet Structures on the Melt Textured Growth YBCO Superconductors

Inki Hong, Hyunseok Hwang, Yung-Hee Han, Sang-Chul Han, Tae-Hyun Sung, and Kwangsoo No

***Abstract*—Melt textured growth YBCO superconductors were fabricated by the top seeding method using Sm1.8 ($Sm_{1.8}Ba_{2.4}Cu_{3.4}O_{7-x}$) seed. The relationship between the Y211 particles and the platelet structures was investigated by micro-structural analysis using SEM. The microstructures of melt textured YBCO superconductors have been examined by TEM and HRTEM. The results of TEM studies clarified the direction of crystal growth and a variety of micro-defects such as twin structures and stacking faults that might behave as pinning centers. Our studies were focused on the stacking faults among those micro-defects by HRTEM and formation mechanism of the stacking faults was studied. The stacking faults formed during the tetragonal to orthorhombic transition that occurred at 450 °C in oxygen annealing. The platelet structures were clearly observed by SEM due to the chemical etching effects. The lengths of stacking faults were increased as the oxygen annealing time increased from 1 hr to 50 hr. The stacking faults were considered to relate to the oxygen contents, as the platelet structures were. The results suggested an oxygen diffusion model for the formation of the stacking faults.**

***Index Terms*—Melt-textured growth, oxygen annealing, platelet structure, stacking fault.**

I. Introduction

FOR practical applications of bulk YBCO superconductors such as a flywheel and bearing system, a large-sized sample having a strong flux pinning force is needed. The melt-textured growth (MTG) technique [1]–[4] is known to be the most promising method of producing $YBa_2Cu_3O_{7-X}$ superconducting materials with a high critical current density (J_c) [5]–[9]. The addition of Y211 is beneficial to J_c enhancement due to the enhanced pinning effect associated with the Y211/Y123 interfaces [10]. Generally, after peritectic heat treatment, oxygen annealing follows at temperatures between 400 °C and 500 °C in an air atmosphere or in flowing oxygen. A possible mechanism is the oxygenation-induced formation of stacking fault during the heat treatment in the oxygen-containing atmosphere. Sung *et al.* first proposed that the CuO stacking faults are formed during low-temperature annealing for the tetragonal-to-orthorhombic phase transition [11]. It has been shown that the lines parallel to the a–b plane are micro cracks formed at the tetragonal–orthorhombic (T–O) transition due to the difference in thermal expansion coefficients between Y123 and Y211 phases [11]. It is known that these stacking faults are occasionally observable in Y123 prepared by standard sintering or melt texturing processes, and they have been characterized both by conventional techniques and by high-resolution imaging. Thus, what is needed is a more complete description of the microstructure, and that is the purpose of the present investigation. The formation of mechanism of the platelet structure is discussed on the basis of the oxygen diffusion mechanism during annealing under flowing oxygen. The most obvious of these defects are stacking faults (double Cu–O layers) [12], [13]. The large number of such stacking faults suggests that some aspect of the fault, such as the partial dislocation at its border, may be acting as a pinning site. Other investigators have made the same suggestion based on transmission electron microscopy (TEM) observations of thin-film samples [14]. High-resolution imaging has shown them to be double Cu–O layers between the Ba–O layers [15]. Recently, evidence has been presented that the deliberate introduction of stacking faults into the Y123 phases through processing techniques results in a higher critical current density.

II. Sample Preparation and Oxygen Annealing

For this experiment 1 mole $YBa_2Cu_3O_{7-Y}$ and 0.4 mole Y_2BaCuo_5, which were prepared through the solid state reaction of Y_2O_3, BaO and CuO powders, were mixed with 0.5 wt% CeO_2 powder. A single crystal of $SmBa_2Cu_3O_{7-X}$ (Sm123) was used as a seed crystal (2 mm × 2 mm × 1 mm). The single crystals were cut parallel to the growth axis into (001) oriented samples, which were polished on both sides. The oxygen diffusion into the Y123 phase is dependent on both the sample size and the internal microstructure of the sample as regards the oxygen annealing [16], [17]. Therefore, the surface of the sample was divided into 2 mm × 2 mm size sections to reduce the annealing time. The samples were annealed in flowing oxygen at temperatures between 450 °C and 500 °C for 1, 3, 10, and 50 hours, respectively. The crystal structures of YBCO single crystals were investigated by means of X-ray powder diffraction. After polishing by DP-paste solutions ($9\ \mu \rightarrow 6\ \mu \rightarrow 3\ \mu \rightarrow 1\ \mu$), we etched the surfaces of the samples using a dilute HCl solution. STEM (Scanning Transmission Electron Microscopy, Philips, CM30) and SEM (Scanning Electron Microscopy, Philips) were used to investigate the microstructure of the textured YBCO superconductor.

Manuscript received August 6, 2002. This work was supported in part by the KEPRI (Korea Electric Power Research Institute), Republic of Korea. This work was supported by a grant from the Center for 10MJ Superconducting Flywheel Energy Storage System, Korea Electric Power Research Institute (KEPRI) and the Center for Applied Superconductivity Technology of the 21st Century Frontier R&D Program funded by the Ministry of Science and Technology, Republic of Korea.

I. Hong, H. Hwang, and K. No are with the Electronic and Optical Materials Laboratory, Department of Materials Science and Engineering, Korea Advanced Institute of Science and Technology, Taejon 305-701, South Korea (e-mail: ink@kaist.ac.kr; musica1@kaist.ac.kr).

Y.-H. Han, S.-C. Han and T.-H. Sung are with the Center for Power Distribution Technology Power System Laboratory, Korea Electric Power Research Institute, Taejon, 305-380 South Korea.

Digital Object Identifier 10.1109/TASC.2003.812131

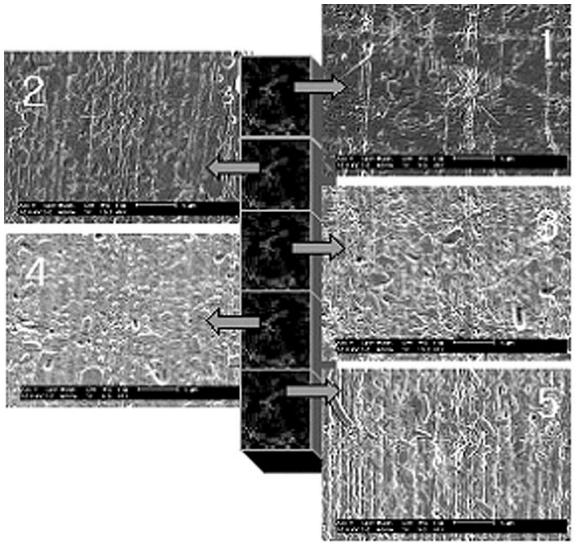

Fig. 1. These samples are chosen at an arbitrary distance from the seed. These surface images are normal on the ab-plane.

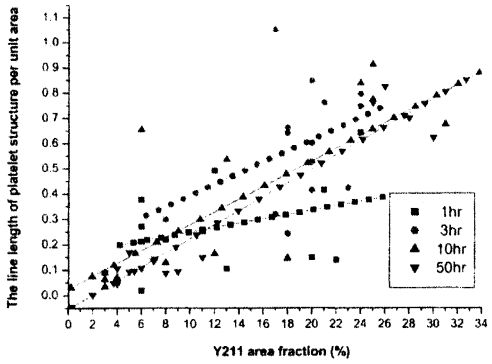

Fig. 2. Relationship between the area fraction of Y211 particles and the platelet structure length per unit area (μm^{-1}) using a linear plot method.

J_c was measured by hysteretic magnetization using a SQUID (Superconducting QUantum Interference Device, Quantum MPMS-7).

III. Microstructures of Melt-Textured YBCO Superconductor

A. Relationship Between the Y211 Particles and the Platelet Structure

Generally, platelet structure was generated by oxygen annealing in the Y123/Y211 interface. We observed the ab-plane samples using SEM (Fig. 1). Furthermore, for each annealing time we examined the total length of the platelet structure and that value was divided into the total area. We calculated the Y211 area fraction in the platelet structure region. We represent the results using a linear plot method in Figs. 2 and 3.

We found that the slopes increased as annealing time was increased. We investigated the relationship between Y211 area fraction (%) and the length of platelet structure per unit area at 10, 50 hours (Fig. 4). As the Y211 area fraction (%) was increased the platelet structure density was increased but over the 25% area fraction the platelet structure was degenerated. Therefore, at the 24% Y211 area fraction, we investigated the generation of the platelet structure. When the Y211 area fraction (about 24%) was constant, the platelet structure's density increased (Fig. 5).

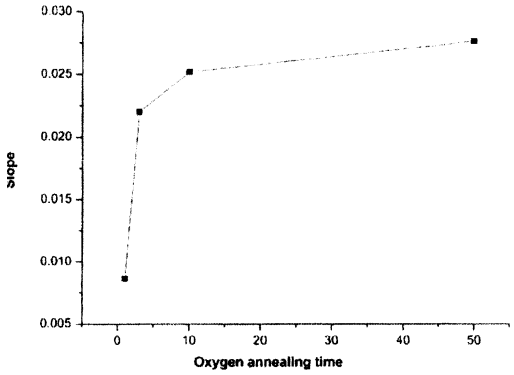

Fig. 3. Relationship between oxygen annealing time and slope on Fig. 2.

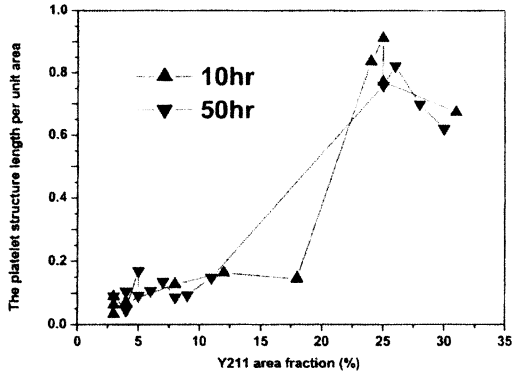

Fig. 4. Relationship between the area fraction of Y211 particles and the platelet structure length per unit area (μm^{-1}).

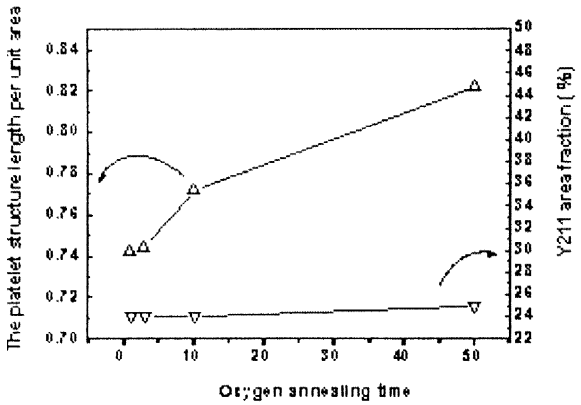

Fig. 5. Relationship between the oxygen annealing time and the platelet structure length per unit area (μm^{-1}) among the constant Y211 area fraction.

B. The Formation of the Stacking Faults During the Oxygen Annealing

After SEM observations, the samples were examined by TEM. TEM observations of samples that were aged in oxygen flow showed strong modifications in the microstructure. When observing micrographs with [001] zone axis, we can easily detect a very large amount of ordered stacking faults near the platelet structure and a progressive decrease of the width of the

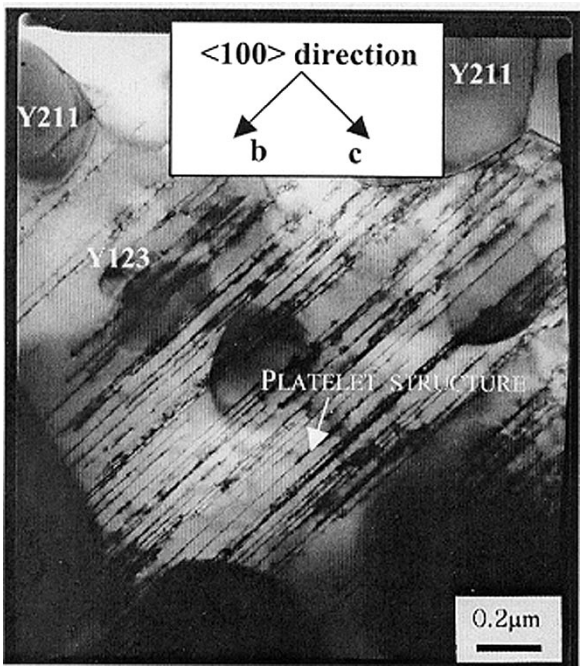

Fig. 6. TEM image of MTG YBCO, which was annealed by oxygen for 1 hour.

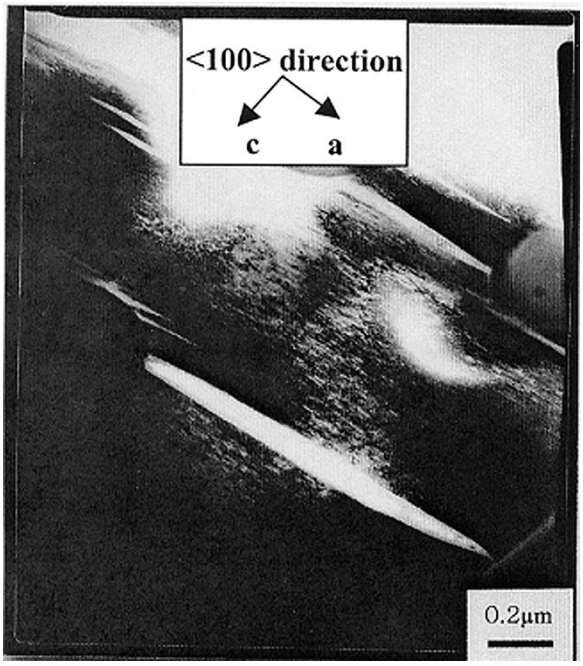

Fig. 7. TEM image of MTG YBCO which was annealed by oxygen during 10 hours.

perturbed area when approaching the Y123/Y211 interfaces. The platelet structures parallel to the *ab*-plane were generated by 1 hour oxygen annealing (Fig. 6). After 3 to 10 hours of oxygen annealing, the amount of the platelet structure increased (Fig. 7). The stacking faults were observed around the Y211/Y123 interface's dark parts and these parts were identified by HRTEM. We examined the stacking faults using an HRTEM image in the 10 hour oxygen annealing sample (Fig. 8).

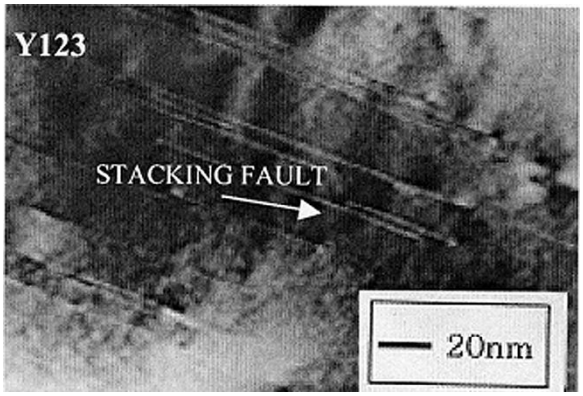

Fig. 8. HRTEM image of MTG YBCO superconductor having oxygen annealing for 10 hours.

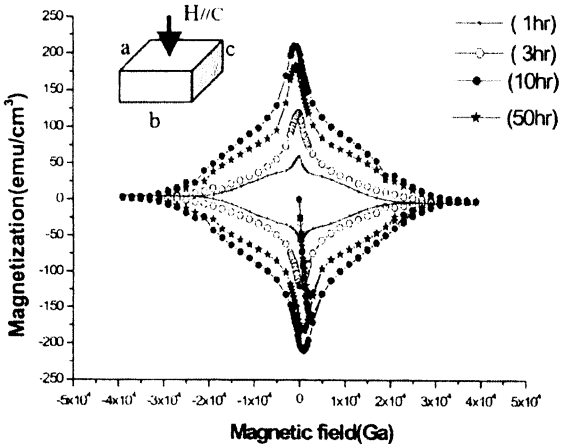

Fig. 9. M–H curve for $H \parallel c$-axis of MTG YBCO crystals at 77 K.

C. Magnetic Measurements

In all cases, the applied magnetic field H was aligned along the c-axis. Measurements were performed to extract the critical current densities, J_c. The $J_c(H)$ curves were derived from the hysteresis loops using the Bean model [18] with the simple formula $J_c(\mathrm{Acm}^{-2}) = [20\,\Delta\, M(\mathrm{emu\ cm}^{-3})]/[b(1-b/3a)(\mathrm{cm})]$, where $\Delta M = (m-)$–$(m+)$ is the width of the loop, and a and b are the large and small lateral dimensions of the crystal, respectively (Fig. 9). We found that the effects of oxygen annealing times increased the values of the magnetizations. However, in the 50 hour oxygen annealing sample the value of $J_c(H)$ curves were derived from the hysteresis loops using the Bean model [18] with the simple formula $J_c(\mathrm{Acm}^{-2}) = [20\Delta M(\mathrm{emu\ cm}^{-3})]/[b(1 - b/3a)(\mathrm{cm})]$, where $\Delta M = (m-)$–$(m+)$ is the width of the loop, and a and b are the large and small lateral dimensions of the crystal, respectively (Fig. 9). We found that the effects of oxygen annealing times increased the values of the magnetizations. However, in the 50 hour oxygen annealing sample the value of J_c was lower than that in the 10 hour oxygen annealing sample. In conclusion, the Y123 decomposition's increase results in the Y123 superconducting phase's decrease. Generally, when the bulk YBCO compound is annealed in the presence of oxygen, the YBCO compound needs 50 hours oxygen annealing but,

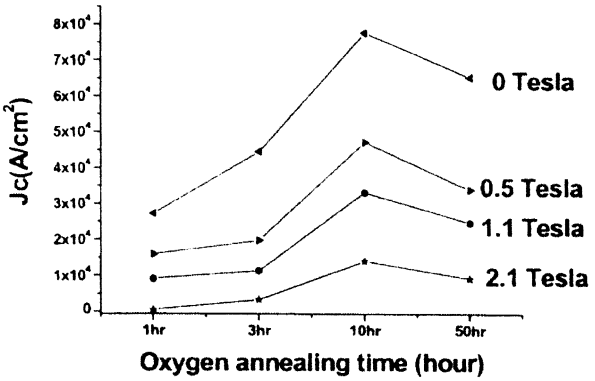

Fig. 10. Oxygen annealing time vs. Critical current density of the MTG YBCO crystals by Bean's critical model.

when the sample sizes of YBCO compounds are very small such as 2 mm $\times$ 2 mm $\times$ 2 mm, the annealing times are changed. In Fig. 10, J_c was increased by the longer oxygen annealing time. In samples having different oxygen annealing times the graph shows an increase. These measurements are in agreement with the observed increase of the platelet structures and stacking faults. In the 50 hour oxygen annealing, however, we found that J_c decreased. This is the reason Y123 phases decrease as the stacking faults are overproduced.

IV. Conclusion

Platelet structures such as $BaCuO_2$ and CuO stacking faults that are present around trapped Y211 particles appear to be formed by decomposition of the Y123 phase during the tetragonal-to-orthorhombic phase transition [19]. The samples of YBCO we observed by SEM and TEM showed platelet structures and stacking faults. The amount of platelet structures and stacking faults were increased as the oxygen annealing times were increased. We measured the increase of J_c using SQUID. Consequently, the increase of J_c is a function of the oxygen annealing time.

References

[1] S. Jin, T. Tiefel, R. Sherwood, R. van Dover, M. Davis, G. Kammlott, and R. Fastnacht, *Phys. Rev. B*, vol. 37, p. 7850, 1988.
[2] T. Meignan, P. J. McGinn, and C. Varanasi, *Supercond. Sci. Technol.*, vol. 10, p. 109, 1997.
[3] P. G. Picard, E. Beaugnon, and R. Tournier, *Physica C*, vol. 276, p. 35, 1997.
[4] Y. A. Jee, G. W. Hong, C. J. Kim, and T. H. Sung, *Supercond. Sci. Technol.*, vol. 11, p. 650, 1998.
[5] C. J. Kim, K. B. Kim, I. H. Kuk, and G. W. Hong, *Physica C*, vol. 255, p. 95, 1995.
[6] K. Salama, V. Selvamanickam, L. Gao, and K. Sun, *Appl. Phys. Lett.*, vol. 54, p. 2352, 1989.
[7] M. Murakami, M. Morita, K. Doi, and K. Miyamoto, *Japan J. Appl. Phys.*, vol. 28, p. L1189, 1989.
[8] Z. Lian, Z. Pingxiang, J. Ping, W. Keguang, W. Jingsong, and W. Xiaozu, *Supercond. Sci. Technol.*, vol. 3, p. 490, 1990.
[9] P. J. McGinn, W. Chen, N. Zhou, M. Lanagan, and U. Balachandran, *Appl. Phys. Lett.*, vol. 57, p. 1455, 1990.
[10] B. Martinez, X. Obradors, A. Gou, V. Gomis, V. Piñol, J. Fontcuberta, and H. Van Tol, *Phys. Rev. B*, vol. 53, p. 2729, 1996.
[11] T. H. Sung, S. H. Han, S. C. Han, H. Choi, O. B. Hyun, J. J. Kim, and M. J. Cima, *Proceed. of the 7th Korea Conference on Mat. and Appl. of Supercon.*, 1997, p. 77.
[12] K. Yamaguchy, M. Murakami, H. Fujimoto, S. Gotoh, Y. Shiohara, N. Koshizuka, and S. Tanaka, *J. Mater. Res.*, vol. 6, p. 1404, 1991.
[13] R. Ramesh, S. Jin, S. Nakahara, and T. H. Tiefel, *Appl. Phys. Lett.*, vol. 57, p. 1458, 1990.
[14] R. Ramesh, D. M. Hwang, J. B. Barner, L. Nazar, T. S. Ravi, A. Inam, B. Dutta, X. D. Wu, and T. Venkatesan, *J. Mater. Res.*, vol. 5, p. 704, 1990.
[15] H. W. Zandbergen, R. Gronsky, K. Wang, and G. Thomas, *Nature*, vol. 331, p. 225, 1988.
[16] C. J. Kim, K. B. Kim, K. W. Lee, C. T. Lee, G. W. Hong, I. S. Chang, and D. Y. Won, *Mater. Lett.*, vol. 11, p. 241, 1991.
[17] C. J. Kim, K. B. Kim, I. S. Chang, D. Y. Won, H. C. Moon, and D. S. Suhr, *J. Mater. Res.*, vol. 7, p. 2349, 1992.
[18] A. M. Campbell and J. E. Evetts, *Adv. Phys.*, vol. 21, p. 199, 1972.
[19] C. J. Kim and G. W. Hong, *Supercond. Sci. Technol.*, vol. 12, p. R39, 1999.